Journal of Manufacturing Engineering, 2009, Vol.4, Issue.2, pp 126-133

COMPARISON OF PREDICTED AND EXPERIMENTAL THERMAL FATIGUE LIVES OF T -91 STEEL TUBE

G.R.Jinu[1], *P.Sathiya[1], A.Rathinam[2] & G.Ravichandran[2]

[1] Department of Production Engineering ,NIT, Tiruchirappalli
[2] Bharat Heavy Electricals Limited,Tiruchirappalli,
.

ABSTRACT

In this paper, a laboratory simulation for reproducing thermal fatigue phenomenon is developed to determine the number of cycles tend to failure occurring in tubes and compared with predicted number of cycles tend to failure using Coffin-Manson equation at a particular temperature. Thermal fatigue test was conducted in Non Destructive Tested T 91 base tube. The tube was subjected to thermal cycles from 800ºC (accelerated temperature) to room temperature. Oxy-acetylene flame was utilised as a heating source, whereas a water bath was utilized for quenching purpose. The test is carried out until open cracks were identified. Surface cracks are identified in the tube after 85 cycles on the heating zone. The tube is then sectioned and subjected to optical microscopy, SEM and EDAX analyses. A comparison of predicted thermal fatigue lives with experimental results shows the deviation of 12 cycles. This study reveals that localised heating and cooling cause's thermal fatigue, which initiates cracks in the tubes.

Keywords: *Thermal fatigue, transverse and circumferential cracks, Coffin-Manson equation*

1. Introduction

ASTM A 213 Gr T-91 steel tubes are widely used in combined –cycle steam systems, because of its greater resistance to the thermal fatigue and enhanced creep, when compared to T22 steel tube. Thermal fatigue is a form of failure that occurs in the components subjected to alternate heating and cooling. These tubes are subjected to the temperature of 600ºC and producing steam at 540ºC and a pressure of 160 bars. Thermal fatigue initially creates crack and eventually failure occurs. The reason for cracking is due to the variation in temperature in the material which induces thermal expansion and contraction. If the surrounding material or any external constraints hinder this expansion, thermal stresses arise. These cyclic thermal stresses cause fatigue similar to that of the mechanical stresses. This type of failures usually occurs in power industries, where turbulent mixing of fluids causes quick thermal transients in boiler heat exchanger tubes [1].

The high temperature superheater and reheater outlets operate at the temperature in excess of 600° C. In a boiler unit, tube expansion may result in fatigue cracks at support attachments, moment restraints the header and stub welds [2]. Failures are reported in critical boiler components subjected to thermal fatigue load applied in pressure vessels [3 & 4].

Virkkunen Iikka et al. [5] conducted experiments on thermal fatigue of austenitic and duplex stainless steels subjected to cyclic thermal transients in the temperature range of 20°C to 600°C. B.B. Kerezsi et al. [6] developed an experimental setup to conduct thermal fatigue using furnace and quenching rig.

Usman et al.[7] analysed the failure of ASTM A 213 Gr T-11 heat exchanger tubes used in ammonia plant which are subjected to thermal fatigue from 850°C to room temperature (25°C). They conducted experiments to confirm the failure results of the site. The experimental result shows the close resemblance with the site results. James P. King et al. [8] has discussed their recent experience in the condition assessment of boiler header components used in fossil fired power plants. It concludes that the failure of headers are due to the material degradation resulting from creep, high temperature headers can also experience thermal and mechanical fatigue. Paterson et al. [9] presented a number of practical examples, where component life monitoring has been implemented on power plants, particularly in high temperature boiler headers and turbines. Headers are subjected to the damage mechanisms of creep due to on load temperatures and pressures. The applicability of the plate to the creep fatigue crack propagation life prediction is examined under high pressure and high thermal stress during plant operations. In-elastic analysis of perforated plate under thermal fatigue are carried out by using finite element method (FEM) and compared with experimental results.

**Corresponding Author- E- mail: psathiya@nitt.edu*

Table 1: Chemical composition of T-91 base tube

Material	Elements (wt %)											
	C	Mn	P	S	Si	Cr	Mo	V	Nb	N	Al	Ni
ASTM A213 grade T-91	0.08-0.12	0.30-0.60	0.020	0.010	0.20-0.50	8.00-9.50	0.85-1.05	0.18-0.25	0.06-0.1	0.030-0.070	0.04	0.04

Smith et al. [11] had simulated a laboratory procedure for reproducing high temperature cracks found in coal fired boiler tubes. They proposed that the crack initiation is due to the intergranular surface corrosion on thermal stress interaction mechanism and environmentally assisted thermal fatigue crack propagation.

From the above literatures, it is clearly found that thermal fatigue is an important phenomenon for the development of crack in pressure vessel components especially in super heater tubes. Many works were already done in studying the influence of thermal fatigue on failure of boiler super heater tubes using FEM and prediction of number of cycles tend to failure occur by various methods. For simulating the thermal fatigue behaviour using laboratory setup is scarce with some constraints (dimensions and other conditions). The objective of this paper is to study the effect of thermal fatigue on T91 base tube and to determine the numbers of cycles tend to failure. In this work, a laboratory simulation for reproducing thermal fatigue phenomenon was developed and the tube was subjected to thermal cycles from 800 ºC to room temperature. The test is carried out until open cracks are identified. The number of cycles tend to failure occur obtained experimentally are compared with the predicted results from Coffin-Manson equation. The cause of the failure is thoroughly investigated in this paper.

2. Experimental Work

2.1 Specimen preparation

One attested ASTM A 213 grade T-91 steel tube of 300 mm length with 48 mm outer diameter. and 10 mm thickness are taken for this experimental study as shown in the Figure1 The chemical composition and the mechanical properties of the T91 tube are given in Table 1 and Table 2 respectively.

Fig.1 T-91 base tube before subjected to thermal fatigue

.

Table 2: Mechanical properties of ASTM A 213 GRADE T-91 material

Material	Ultimate tensile strength, UTS [MPa]	0.2%Yield strength, YS [MPa	% of Elongation
ASTM A 213 Grade T-91	585	415	20

2.2 Experimental set up

The apparatus has been built for conducting thermal fatigue tests. The test set up employed in this study consists of the following main physical components:

1. The Oxy-acetylene heating set up.
2. The specimen mounting frame.
3. The specimen holding system.
4. Quenching rig
5. Laser sensor temperature measuring system.

The specimen is locally heated up by Oxy-acetylene torch from the outer surface of the tube. The peak temperature can be suddenly attained by this process. The experimental set up is shown in figure 2.

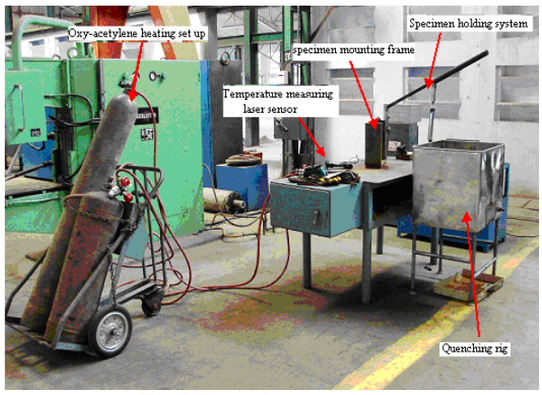

Fig.2 Experimental setup

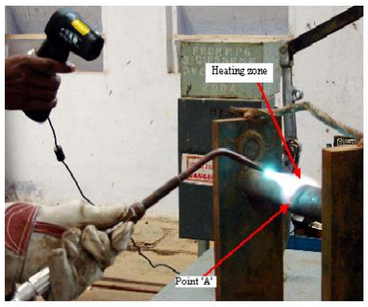

Fig.3 Specimen mounting frame with heating

2.3 Experimental procedure

The specimen is prepared as discussed above and heat is applied from the outer surface of tube which is the actual condition of a heat exchanger tube exposed to the thermal fatigue on pressure vessels. The flame is shown in the heating zone manually, starting from one point of the heating zone and ends in the same point so that heat will be uniformly distributed from the outer surface tube to the inner surface as shown in Figure 3. After heating the temperature of specimen is measured by using laser thermometer to check, whether the attained temperature reaches 800 ºC. The time taken to attain 800 ºC is 7 minutes. The flame is then switched off. Then the hot specimen is lifted with the help of the specimen holding system and immersed into the quenching rig. The specimen is taken out from the quenching rig, when the temperature of the specimen reaches the room temperature. All the above process constitutes one thermal fatigue cycle. For one thermal cycle, the duration of 10 minutes is taken, which includes both the heating and the cooling cycle. The experiments are conducted till open cracks are identified. Surface cracks are identified in the base tube after 85 cycles. The specimen is then removed from the specimen mounting frame and NDT tests are carried out and it is sectioned for metallographic study.

3. Prediction of number of cycles to failure occur using Coffin–Manson equation

Coffin and Manson [12] established that the plastic strain-life data could also be linearised with log–log coordinates. The equations of Basquin and Coffin–Manson hold the stress-based and strain-based fatigue properties, respectively. The summation of these equations is known as Coffin–Manson equation:

$$\frac{\Delta\varepsilon}{2} = \frac{\sigma_f'}{E}(2N_f)^b + \varepsilon_f'(2N_f)^c \qquad (1)$$

Where σ_f' and b are fatigue strength coefficient and fatigue strength exponent, respectively, and the ε_f' and c correspond to fatigue ductility coefficient and fatigue ductility exponent, respectively. N_f denotes the number of cycles to failure. From the above equation-1, the number of cycles tend to failure are calculated. The temperature dependent material properties such as coefficient of linear expansion (α), linear strain and modulus of elasticity are shown in Figure (4, 5 & 6) respectively. Tensile specimens are prepared to conduct high temperature tensile test as shown in Figure 7. This test was carried out to find the fracture stress and fracture strain at 800°C and the obtained stress- displacement graph is shown in Figure 8.
From figure 4, the linear thermal expansion corresponding to 800°C is 13.38×10^{-6} K and the difference in temperature is 800°C (ΔT).

$$\Delta\varepsilon = \alpha\Delta T = 1.07 \times 10^{-2} \qquad (2)$$

Using the above equation-2, the linear strain is found to be 1.07×10^{-2}. From the stress- displacement graph (Figure 8) at 800°C the fracture stress (σ_f') and fracture strain (ε_f') are found to be 100 N/mm^2 and 0.2011 respectively. From Figure 6, the modulus of elasticity (E) for 800°C is 1.55×10^5 MPa. The fatigue strength exponent and fatigue ductility exponent are -0.12 and -0.7. All the above values are substituted in equation (1) and it is identified after 97 cycles, failure will occur.

4. Results and Discussion

For validating the experimental results, the experimentally obtained number of cycles tend to failure are compared with the predicted results from

Coffin–Manson equation. The obtained surface cracks are then subjected to metallographic examination.

4.1 Comparison of predicted results with experimental results

Table 3 shows the comparison of experimental and predicted results and it is identified that a difference of 12 cycles is obtained**.**

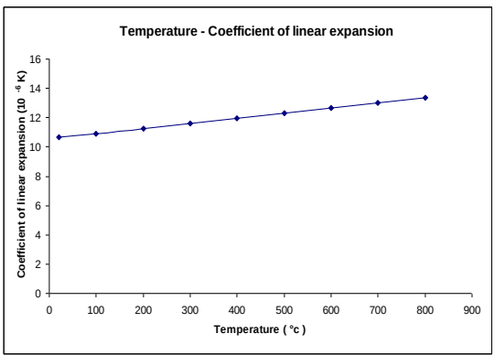

Fig.4 Variation of coefficient of linear expansion with temperature [13]

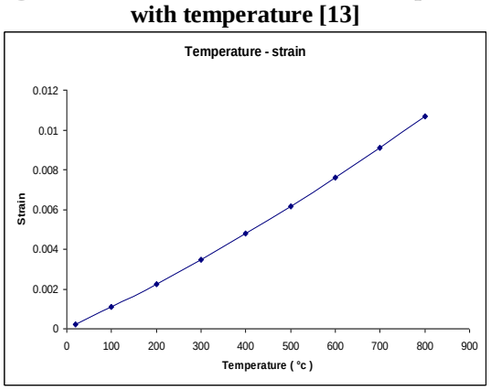

Fig.5 Variation of strain with temperature [13]

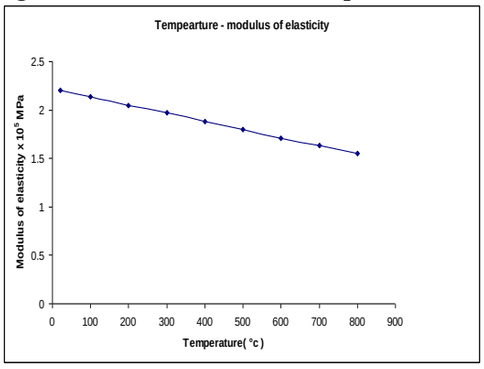

Fig.6 Variation of Modulus of Elasticity with temperature [13]

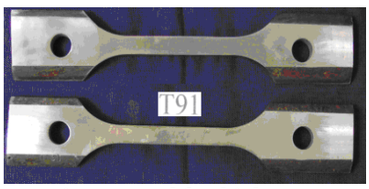

Fig.7 Tensile specimens used for high temperature tensile test

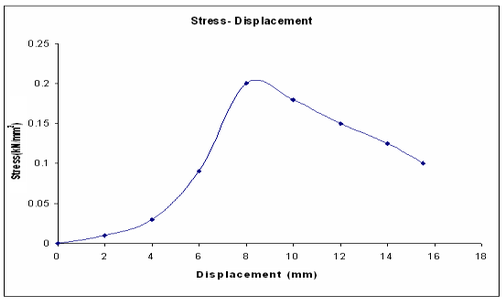

Fig.8 Stress- displacement graph correspondding to 800°c

This shows that the developed experimental set up can produce closer results and the percentage of error is found to be 12.37 %. This deviation is due to variation in the heating and cooling cycle.

Table 3: Comparison of experimental and predicted results

Predicted number of cycles tend to failure	Experimentally identified number of cycles tend to failure	Difference in number of cycles	% of deviation
97	85	12	12.37

4.2 Metallographic examination of the obtained surface crack

The obtained surface cracks are subjected to metallographic examination to study the crack in detail. The failed base tube is subjected to visual examination and liquid penetrant test, to study the surface cracks. Then the tube is sectioned and subjected to micro, macro and SEM study to deal with the crack in detail.

4.2.1. Visual inspection in failed base metal tube

The macrograph of the failed base metal tube is shown in figure 9. From figure 9, it is observed that

lot of surface cracks are obtained in the tube subjected to thermal fatigue after 85 cycles.

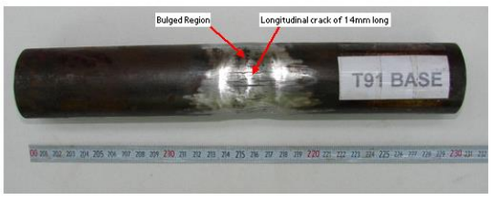

Fig.9 Visual inspection of failed base metal

A 14mm long longitudinal crack is visually identified in the failed base tube at the heated zone. The tube becomes bulged in the heating zone, which is clearly seen. The failed tube is then subjected to liquid penetrant test in order identify the small surface cracks.

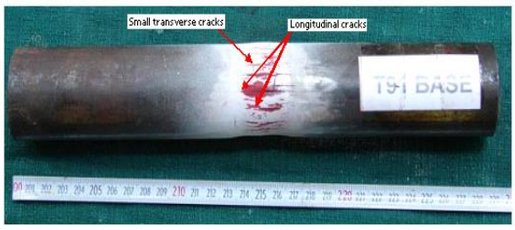

Fig.10 Liquid penetrant examination of failed base specimen

4.2.2 Liquid penetrant test on failed base metal tube

The macrograph of the failed base metal tube specimen is subjected to liquid penetrant test, to identify the small surface cracks is shown in Figure 10. It clearly shows that lot of longitudinal cracks is found in the heated zone and from the longitudinal crack small transverse cracks are also identified, which are invisible in the visual examination. The failed tube is then sectioned and subjected to metallographic study.

4.2.3 Specimen preparation for metallographic study

The sectioned view of the failed base tube is shown in Figure 11. The failed tube is sectioned into two halves in longitudinal direction and again one half of the tube was divided into two sections. The projected portion from the two sides of the heating zone in the tube was removed further so that only the heated zone is taken for metallographic study. Specimens for metallographic examinations were prepared by polishing successively in 220, 320, 400, 600, 800 emery grits, followed by a cloth disc polishing. The specimens were etched with 10% Nital solution. The specimen is studied through microscope, SEM and EDAX analyses the results were discussed.

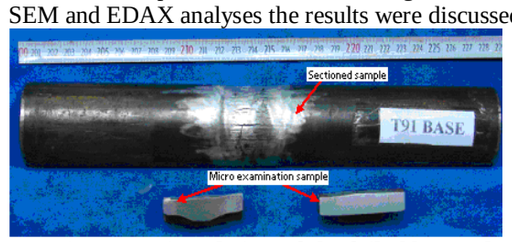

Fig.11 Sectioned view of the failed base tube

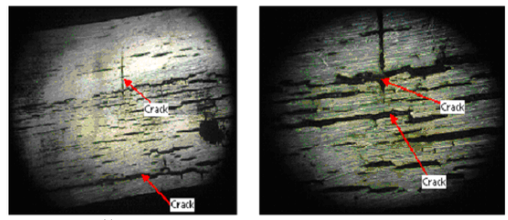

Fig.12 Magnified view of the surface crack obtained in the failed base tube

4.2.4. Macro study on the failed base metal tube

Before subjecting to the micro analysis the polished sample is subjected to macro study. The macro photographs are taken in the outer surface of the failed tube to get the closer view of the cracks obtained in the surface, while the micro structure is taken in the cross-section of the failed tube on the thickness side to study the depth of penetration of the crack. Figure 12 (a) shows the magnified view of the surface crack obtained in the failed base metal tube subjected to thermal fatigue and it is clearly identified that a lot of longitudinal cracks are developed in the heated zone and from the longitudinal crack small transverse cracks are also observed. Figure 12 (b) shows the magnified view of the single longitudinal crack obtained in the failed base metal tube.

4.2.5 Optical microscopy

The samples were prepared. The polished and etched samples were examined under optical microscopy and SEM. The micro structures are taken in different locations of the tube with defect and defect free surfaces.

4.2.5.1 Study on the defect free surfaces on the failed base metal tube

The microstructures of defect free surfaces of the failed base tube are shown in figure 13. The figure shows that the grain size is larger. The dark coloured

grains seen in the microstructure are the tempered martensite. The tempered martensite gives high creep strength at elevated temperatures. The large grain size also helps in preventing cracks. The carbides and carbo nitrides formed are found on the grain boundaries.

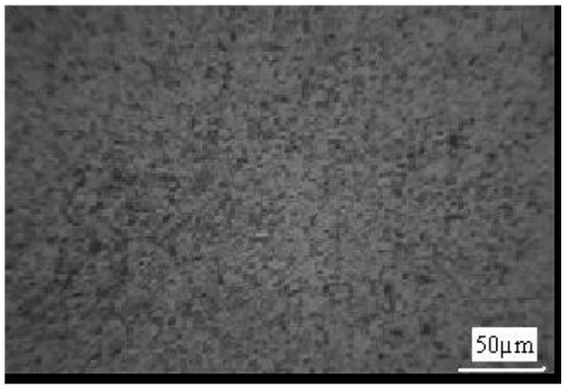

Fig.13 Microstructure of base in defect free region Higher hardness is due to the result of the tempered martensite and the carbides

4.2.5.2 Study on the defect surfaces on the failed base metal tube

Through the optical microscope, the defect surfaces in the T91 base metal tube were identified and presented in figure 14 (a -d). From the figure 14 (a-c) it is clearly identified that large number of cracks was found in the failed base tube and figure 14(d) shows that voids like defects are also found. The cracks are developed from the heating surface (outer surface) of the tube and propagated towards the inner surface. Cracks and voids observed in the failed base tube are similar to the cracks observed in the failed tubes [8].

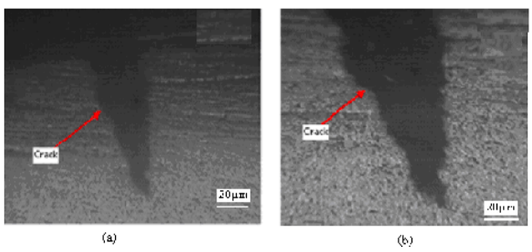

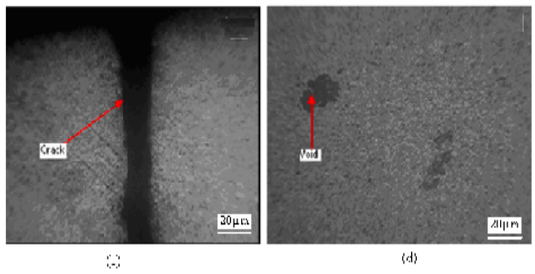

Fig.14 (a-d) Cracks and voids identified in the failed base tube

4.2.6 SEM study

The cracks and voids observed in the optical microscope are subjected to SEM study to analyse the failures in detail. SEM analyses are carried out in defective surfaces of the base tube. The cracks observed in the SEM examination ofthe failed base tube are shown in figure 15(a-b). The cracks develop from the outer surface of the tube and propagate towards the inner surface. Similarly, it occurs in the circumference of the heated region of the tube. Micro – void formation is observed inside the cracked surface at higher magnification and it is clearly shown in figure 16 (a-b). When the cracked surface is further magnified, grain boundary cracks are also observed as shown in Figure 17. From figure 15 (a-b), it is clearly identified that the initial position of the crack width is high, while observing towards the inner surface, the growth rate of the crack increases due to the difference in temperature and rate of cooling. Due to this reasons cracks and voids are developed.

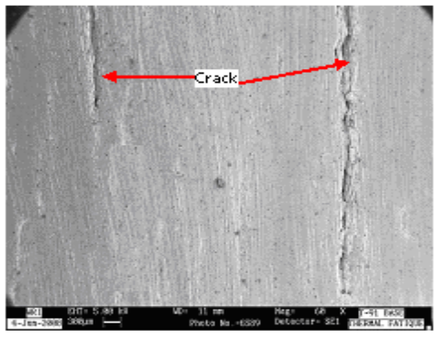

(a)

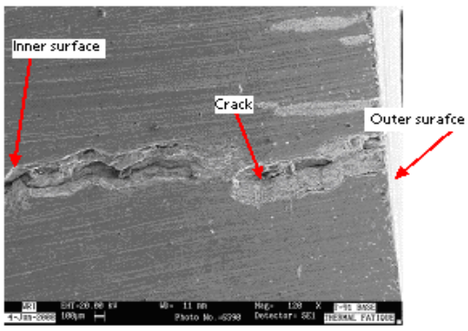

(b)

Fig.15 (a & b) Crack propagation in the failed base tube

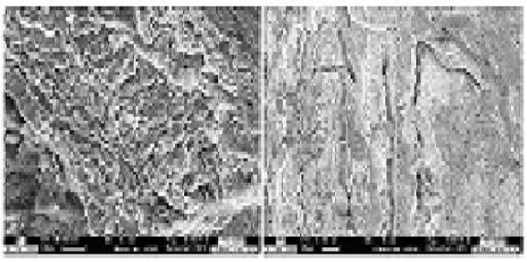

(a) (b)

Fig.16 (a&b) Grain boundary micro-void formation inside the crack

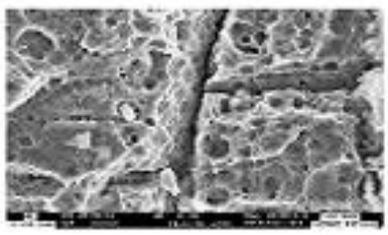

Fig.17 Cracking along the grain boundaries

On evaluating the micro study and SEM results, it is clearly observed that the cracks are developed from the heating surface (outer surface) of the tube and propagates towards the inner surfaces, which eventually cause failure of the tube. The cracks occurred in the tube is due to long time exposure in service temperature. Grain boundary cracks and micro – void formation is also observed inside the crack at higher magnification. The voids and cracks obtained in the tube specimen is the typical thermal fatigue crack, which is similar to the failures reported in tubes, subjected to thermal fatigue [8].

Table 4: Hardness taken in the base tube

Position	Base	heating zone	near the crack
Before subjected thermal fatigue	212, 210	_	_
After failure occurs	284, 282	383, 376	483, 429

4.2.7. EDAX analyses

The EDAX analyses are carried out separately on the specimens before subjected to thermal fatigue and after failure occur; in order to identify any foreign elemental segregation occurs during thermal cycling. The EDAX spectrum of the base and failed specimens are shown in figure 18 (a - b).

From the spectrums and elemental results, it is found that both the base and failed specimens have the same spectrum which indicates the failure in not due to the segregation of any foreign elements during thermal cycling. The failure is due to the grain boundary crack as identified in SEM results, which is a typical thermal fatigue failure.

(a) Before thermal fatigue

Fig.18 (a & b) EDAX analyses of base and failed samples

4.2.8 Hardness

Vickers's hardness measurements are taken in the base tube material before subjected to thermal fatigue and after the failure. The hardness location taken in the base specimen is shown in Figure 19. The load applied was 10 kg and the hardness values taken in the base tube material are noted in table 4.

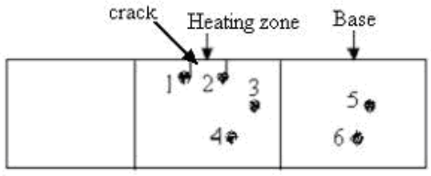

Fig.19 Hardness locations taken in the failed base tube

From table 4, the hardness value is much greater, nearer to crack zone. Due to the higher hardness the initiated cracks caused due to the thermal fatigue are propagated towards the circumferential areas and through the thickness of the tube. Due to repeated heating and cooling, the grains get finer and the hardness values get increased, when compared to the base material.

5. Conclusion

From this research work, the following conclusions are drawn, The effects of thermal fatigue on ASTM A 213 GRADE T-91 base tube is studied effectively and the number of cycles tend to failure are obtained experimentally are compared with predicted fatigue lives obtained from Coffin-Manson equation. While thermal cycling (at 800°C), surface cracks are identified experimentally in the base tube after 85 cycles and using Coffin-Manson equation, it is predicted that failure occurs in the tube at 97 cycles. The comparison of the experimental and the predicted results shows the difference of 12 cycles. This reveals that the developed experimental setup can produce closer results and the percentage of error is found to be 12.37 %. This deviation is due to the variation in heating and cooling cycle. From the visual examination, 14mm longitudinal crack is visually identified in the failed base tube at the heated zone. Liquid penetrant test result reveals that apart from the longitudinal crack, small transverse crack are also observed in the failed base tube.

From the macro and the micro examinations cracks and voids are observed. The cracks develop from the outer surface of the tube and propagate towards the inner surface of the tube. In the SEM examination, the grain boundary cracks and micro – void formation are observed at higher magnification. The EDAX analyses reveals that the cracks developed are not due to the segregation of any foreign elements during heating and cooling cycle. The failure is due to the grain boundary crack as identified in SEM results, which is a typical thermal fatigue failure. The hardness test shows that the point nearer to the crack the hardness value is much higher. Due to the higher hardness cracks developed by the thermal fatigue process propagate towards the circumferential areas and through the thickness of the tube by thermal fatigue process. The development of these cracks is due to the temperature variation from high temperature to room temperature, which is similar in the power plant during the start up and shut down operations.

References

1. *Hayashi.M, Thermal fatigue behavior of thin walled cylindrical carbon steel specimens in simulated BWR environment. Nuclear Engineering and Design, Vol. 184, 123 – 133, 1998.*
2. *Yoshimoto.T, Ishihara. S, Goshima.T, McEvily.A.J & Ishizaki.T. An improved method for the determination of the maximum thermal stress induced during a quench test. Scripta Materialia, Vol. 41 (5), 553 – 559, 1999.*
3. *Tulyakov GA. Thermal fatigue in heat power engineering, Mashinostroyeniye, 1978.*
4. *Vainman.A.B, Melekhov.R.K & Smiyan.O.D. Hydrogen induced embitterment of high- pressure boiler elements. Kyiv: Naukova Dumka, 1990. .*
5. *Virkkunen Iikka. Thermal fatigue of austenitic and duplex stainless steels. Acta Polytechnica Scandinavica, Published by the Finnish Academies of Technology Mechanical Engineering Series No. 154, Espoo2001.*
6. *Kerezsi .B.B, Price. J.W.H, Ibrahim.R.N., repeated thermal shock (Journal of Materials Using S–N curves to analyse cracking due to Processing Technology) Vol.145,118–125,2004.*
7. *Usman.A, Nusair Khan.A, Failure analysis of heat exchanger tubes, (Engineering Failure Analysis) vol. 15, 118-128, 2001.*
8. *James.P. King DB Riley, Inc. Worcester, Massachusetts, Recent experience in condition assessments of boiler header components and supports, Presented at the1996 ASME Pressure Vessels and Piping Conference 21-26, 1996.*
9. *Paterson .I.R., Wilson .J.D., Use of damage monitoring systems for component life optimisation in power plant (International Journal of Pressure Vessels and Piping), Vol. 79, 541–547, 2002 .*
10. *Takumi tokiyoshi, fumiko kawashima, toshihide isari, hironori kino ,crack propogation life prediction of a perforated plate under thermal (International Journal of Pressure Vessels and Piping) vol. 78 (2001.) p .837–845.*
11. *Smith B. J, Erskine. C.I., Hartranft.R. J, and Marder.A.R., High-Temperature Corrosion-Fatigue (Circumferential) Cracking life Evaluation Procedure for low Alloy Cr-Mo) Boiler Tube Steels, , PA 18025*
12. *Coffin, L. F., "Fatigue at High Temperature," in Fatigue at Elevated Temperature, ASTM STP 520, American Society for Testing and Materials, 5-34, 1973.*
13. *JC.Vailant, B.Vandenberghe, C.Zakin, The T91 / P91 book, Vallourec & Mannesmann tubes, 2006.*